INTERNATIONAL JOURNAL OF OPTIMIZATION IN CIVIL ENGINEERING
Int. J. Optim. Civil Eng., 2022; 12(3):435-455

DEVELOPMENT OF NEURAL NETWORK MODELS TO ESTIMATE LATERAL-DISTORTIONAL BUCKLING RESISTANCE OF CELLULAR STEEL BEAMS

A. Moghbeli, M. Hosseinpour and Y. Sharifi[*, †]
Department of Civil Engineering, Vali-e-Asr University of Rafsanjan, Rafsanjan, Iran

ABSTRACT

The lateral-torsional buckling (LTB) strength of cellular steel girders that were subjected to web distortion was rarely examined. Since no formulation has been presented for predicting the capacity of such beams, in the current paper an extensive numerical investigation containing 660 specimens was modeled using finite element analysis (FEA) to consider the ultimate lateral-distortional buckling (LDB) strength of such members. Then, a reliable algorithm based on the artificial neural networks (ANNs) was developed and the most accurate model was chosen to derive an efficient formula to evaluate the LDB capacity of steel cellular beams. The input and target data required in the ANN models were provided using the ANN analyzes. An attempt was made to include the proposed formula in all the variables affecting the LDB of cellular steel beams. In the next step, the validity of the proposed formula was proved by several statistical criteria, and also the most influential input variable was discussed. eventually, a comparison study was executed between the results provided by the ANN-based equation and the AS4100, EC3, and AISC codes. It was revealed that the presented equation is accurate enough and can be used by practical engineers.

Keywords: cellular steel beams; ANN; LDB; FEA; The AS4100, EC3, and AISC codes

Received: 10 January 2022; Accepted: 15 May 2022

[*]Corresponding author: Department of Civil Engineering, Vali-e-Asr University of Rafsanjan, Rafsanjan, Iran
[†]E-mail address: y.sharifi@vru.ac.ir (Y. Sharifi)

1. INTRODUCTION

A cellular steel beam is produced by welding two complementary parts of I-section beams. This type of beam is manufactured by cutting the cross of the beam semicircularly then the cut pieces are welded together with a certain shift (Fig. 1). According to this, the depth of the cellular beam increases by 40 to 60% compared to the depth of its former section, which makes it perform better under bending. These types of beams are liable to several types of failure modes due to the opening in their web these openings complicate flexural-shear instabilities. These modes comprise flexural, Vierendeel, shear, LTB, LDB, web buckling, or a combination of a number of these modes.

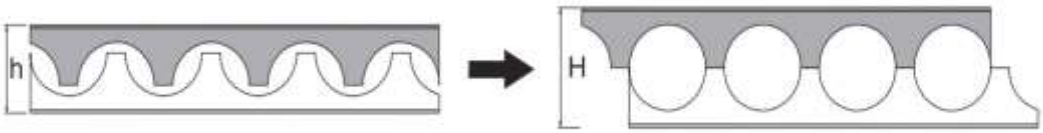

Figure 1. The fabrication process of cellular steel beams

The buckling behavior of thin-walled steel sections is extremely important in their analysis due to the sudden buckling that occurs. The slender beams with web openings have many applications, and since their depth is greater than conventional I-shaped sections without web openings, they are more likely to collapse in the LTB failure mode [1-3]. Although in some previous research, the LTB failure of cellular steel beams has been studied [4-7] but less attention is paid to the LDB failure mode and its characteristics are poorly examined. Previously, the common failure modes of cellular steel beams have been studied. The main design formulae for these modes can be seen in Ref. [8–12]. Moreover, some researchers examined the effects of the geometric properties of cellular steel beams on the LTB mode [13–15]. The LTB mode is more common in long-span beams, while local buckling is more common in short-span beams, but for beams with intermediate span length, the interaction of the abovementioned modes yields a new failure mode, named the LDB. This mode is characterized by simultaneous twists, lateral displacement, and web distortion [16-24]. Distortion buckling occurs in two different manners; “LDB” and “restrained distortional buckling (RDB)” (Fig. 2). RDB mode may take place when the tension flange is prohibited from torsion and lateral displacement, for example in the negative moment part in a composite beam or a half-through bridge girder.

Bradford [21], and Zirakian [22] tested a series of steel I-beam specimens experimentally and the LDB failure of such beams was investigated. Moreover, Zirakian and Showkati [23] examined the LDB failure mode of the castellated steel beams; but, so far, very few experimental tests have been carried out on the LDB behavior of cellular beams.

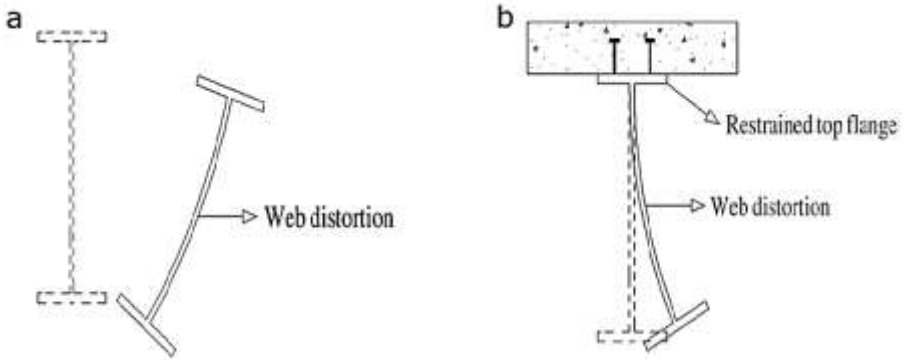

Figure 2. Distortion buckling failure modes: (a) LDB, (b) RDB

The ANN is introduced as a system that solves complicated problems that do not solve using existing continuous algorithms. In the last decades, engineers carried out special studies addressing different problems utilizing ANN with various degrees of success. They utilized ANN to solve the problems in the field of material performance, structural identifications, geotechnical, transportation, construction management, heat and fluid problems, electronics and control, and infrastructure issues [25-34].

The purpose of the present paper is divided into two parts: simulation of models based on the FEA for cellular steel beams subject to buckling, and development of accurate ANN models in order to derive a precise formula for evaluating the LDB capacity of such beams. The reliable database needed for the ANN training was obtained from the FEA using ABAQUS software [35]. The ABAQUS software considers inelastic material properties as well as initial geometry imperfections. A series of 660 FEA models under LDB failure mode was analyzed using a high-speed computer. Validation of numerical results was confirmed by experimental tests. The ANN method was then used to develop an empirical formula for predicting the LDB moment of cellular steel beams. First, all parameters that might affect the ultimate LDB strength of cellular beams were predicted, and then by performing a sensitivity analysis, the effective parameters were selected. Then, the relationship between these effective parameters and the ultimate resistance of cellular beams was recognized through proper training of ANN and a new equation was proposed. Finally, the predicted outcomes attained from the ANN-based formula were compared to the design capacities obtained from AISC [36], AS4100 [37], and Eurocode3 [38]. So far, no study has been found that deals with the LDB failure mode in cellular steel beams, which is attempted in the current study.

2. FE MODELING

Numerical studies present a reliable and safe understanding of the behavior of structural elements and to date, it has been widely used by researchers. As mentioned early, one of the main objectives of this research is considering the LDB performance of the cellular steel girders utilizing the FE approach. Here, using ABAQUS software, 3D models were employed to simulate the real behavior of the cellular steel beams especially material and

geometry nonlinearities. The Eigenvalue analysis was first performed to evaluate buckling modes. Then, the output results obtained from the Eigenvalue analysis adopted for the second step of the analysis named RIKS analysis in the ABAQUS library, which is a nonlinear load-displacement analysis. A full Newton-Raphson procedure, as well as an Arc Length Control Iterative, was used for solving the nonlinear equations. The Doubly curved shell elements including 3-node (S3R) and 4-node (S4R) were utilized to model. The quantities of Poisson's ratio and modulus of elasticity were adjusted as 0.3 and 2e5 MPa, respectively. the fabrication procedures of cellular steel beams made us exert an initial geometric imperfection. Based on the AS4100 code recommendation [37], a tolerance of $L_b/1000$ for flexural elements was recommended, where L_b refers to the length between lateral bracing.

2.1 Validation of numerical models

In order to confirm the results of FEA-based models, the results of experimental research conducted by two separate studies with different boundary conditions were used. The simply supported beams with an I-shaped section and subjected to concentrated load were tested by Zirakian and Showkati [39], they considered different geometries and examined the LDB resistance and failure modes. Moreover, I-shaped beams that prevented the displacement of their compression zones were studied by Bradford and Wee [40], and their buckling behavior was experimentally examined. From each of the two mentioned studies, a beam was numerically modeled and the obtained results were compared to the experimental results. As can be seen from Table 1, despite the different boundary conditions in the modeled beams, the error percentage of the results is less than 2% and the developed FE models are well able to predict the ultimate LDB resistance. Further, Fig.3 illustrated the deformed shape of the numerical and experimental tests, which is a good match between them.

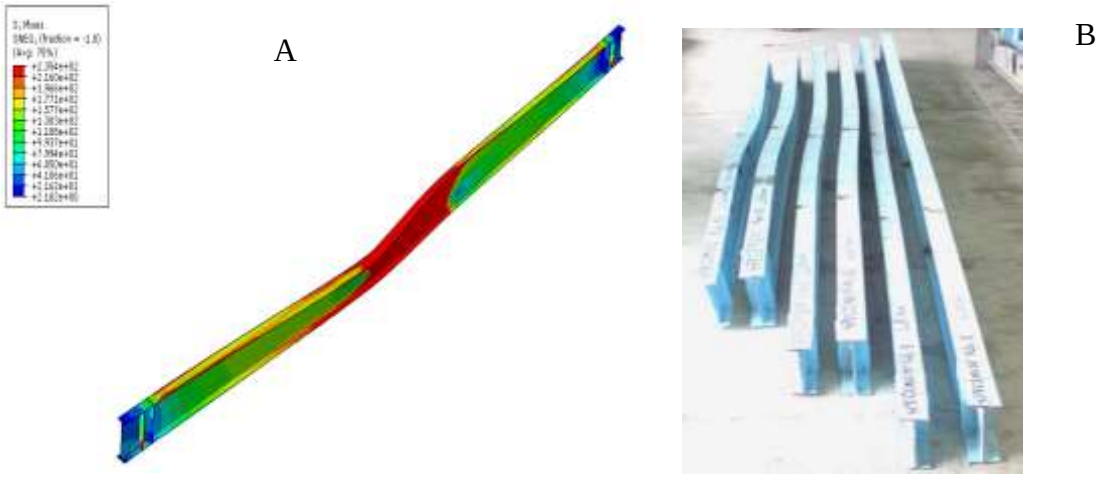

Figure 3. Deformed shape of A) FEA model, B) Experimental test [39]

Table 1: Comparison between test and FE results

Model	L_b (mm)	t_f (mm)	t_w (mm)	b_f (mm)	d (mm)	P_{EXP} (kN)	P_{FEA}(kN)	*Err* (%)
s-180-4400 [39]	3600	6.3	4.85	64	180	22.35	21.96	1.77
B-1 [40]	2700	10	6	90	175	50.1	49.63	0.95

2.2 Parametric study

According to the numerical model validated in the previous section, an extensive parametric study was performed, including 660 samples with the boundary conditions illustrated in Fig. 5. The range and statistics related to the geometric properties and ultimate distortional buckling (M_{DB}) of the numerical models are reported in Table 2 to determine the extent of the parametric study. The beam geometry parameters listed in the table are displayed in Fig. 4. Furthermore, it should be noted that the different ratios specified in Table 2 correspond to the input and output variables of the ANN models, which are discussed in the following sections.

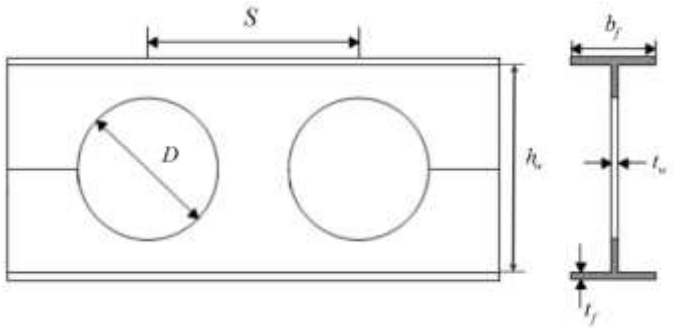

Figure 4. Beam and cellular geometry

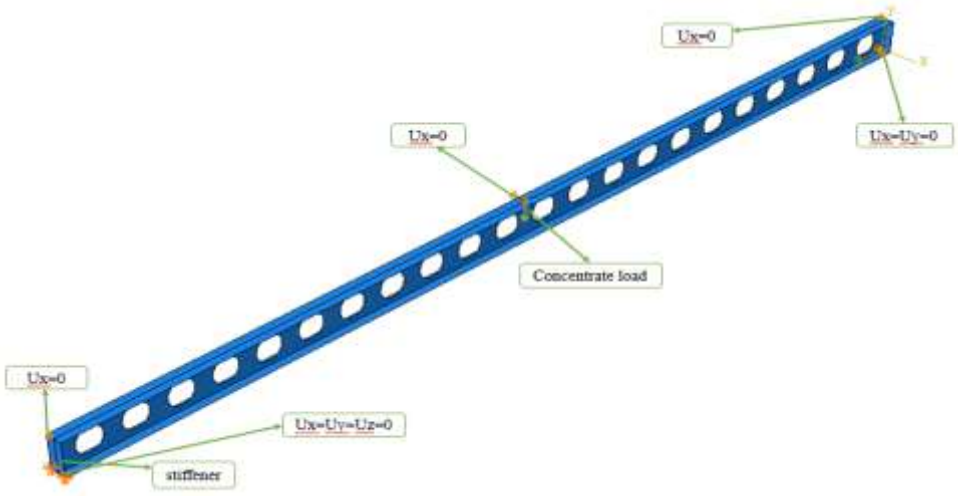

Figure 5. Boundary conditions in finite element models

Table 2: The statistical parameters of the input random variables.

	$\frac{h_w}{b_w}$	$\frac{t_f}{t_w}$	$\frac{h_w}{t_w}$	$\frac{b_f}{2t_f}$	$\frac{L_b}{r_y}$	$\frac{h_w}{D}$	$\frac{S}{D}$	$\frac{E}{F_y}$	$\frac{M_{DB}}{M_P}$
Median	2.595	1.657	57.385	6.445	148.807	1.313	1.461	579.710	0.747
Mode	2.510	1.600	49.85	5.920	111.750	1.210	1.460	444.440	0.380
Std. Deviation	0.431	0.057	7.735	0.710	19.742	0.085	0.081	146.643	0.132
Variance	0.186	0.003	59.824	0.504	389.732	0.007	0.007	21504.16	0.017
Skewness	0.474	0.691	-0.105	0.917	-0.001	0.465	0.130	0.284	-0.605
Kurtosis	-0.233	-0.495	-0.687	-0.599	-1.042	-0.542	0.104	-1.502	-0.789
Range	1.860	0.180	31.460	2.170	75.630	0.360	0.450	355.56	0.530
Minimum	1.820	1.600	40.770	5.920	111.750	1.180	1.240	444.440	0.380
Maximum	3.680	1.780	72.230	8.090	187.370	1.540	1.680	800.000	0.910

3. LDB EQUATIONS

Not only there is no suitable formulation for evaluating the LDB capacity of intact steel beams but also the LDB capacity of cellular steel beams is more complicated. The only design assessment was suggested by the AISC [36], AS4100 [37], and EC3 [38] that employed for LTB of doubly symmetric I-sections. Fig. 6, shows the compassion between the results of LDB capacity using FEA and the results of the LTB solution of the mentioned codes. Based on the results provided in Fig. 6, it can be found that the code provisions are not able to assess the LDB capacity of cellular steel beams exactly and the M_u/M_{FEA} ratio has a large dispersion for all three codes. Therefore, further studies are required to improve the LDB scenario and a formula-based approach to cellular steel I-section beams.

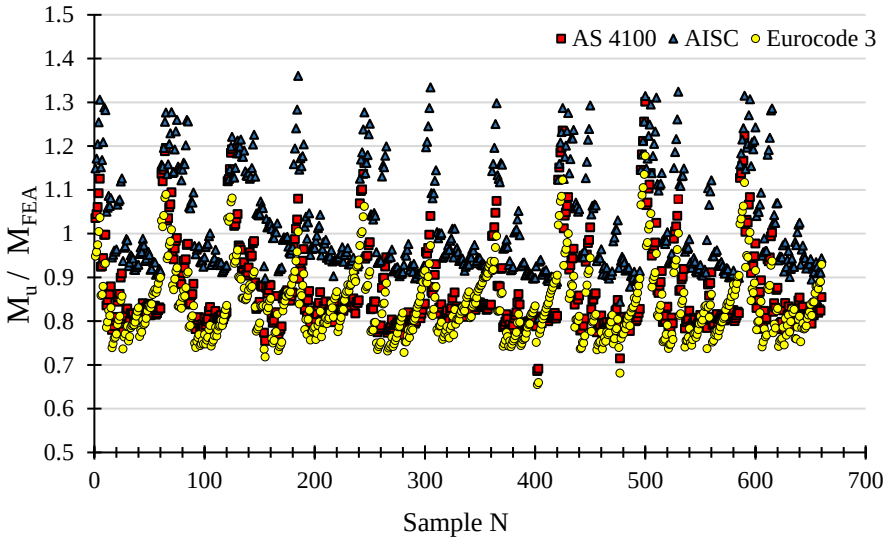

Figure 6. The ratio of the buckling load obtained by FE and code solutions

4. ARTIFICIAL NEURAL NETWORK

As mentioned before, the most important purpose of the current study is to use neural networks to propose a new practical formula for calculating the LDB strength of cellular I-beams. ،Therefore, an ANN model was developed and relationships between the parameters affecting the LDB strength of cellular I-beams were acquired through the developed model. In the following, the first, the general function and structure of a multilayer perceptron ANN model are discussed, and next the final developed ANN model for estimating the ultimate strength of cellular beams, as well as its corresponding formula, is presented.

4.1 Structure of a multilayer perceptron ANN model

The artificial neural network is known as a powerful mathematical technique that simulates the biological form and behavior of neurons, and the multilayer perceptron (MLP) is known as one of the most popular neural networks. The MLP is suitable for examining any continuous function with desirable accuracy. This class of neural networks employs a feed-forward procedure; the feed-forward procedure predicts one or more variables as network outputs using predictor input variables. This procedure is based on layers that are connected to each other by synapses. Each synapse has a weight that indicates the influence of the neuron. The procedure is called feed-forward since it has no feedback loops and the network connections move from the input layer to the output layer [41]. Moreover, a supervised back-propagation (BP) learning algorithm, is employed for multi-layered networks. This learning process is one of the most typical settings in neural networks. According to this algorithm, a comparison is made between the target output and the expected output, and the weights are adjusted based on that. The beck-propagation algorithm is employed to optimize the networks by minimizing the simulation error to an expected value [42].

Mostly, the technique of trial and error is employed in order to reach the configuration of an ANN model. Fig. 7 illustrates the typical configuration of a simple shallow ANN model with one hidden layer. The number of nodes in the input and output layers is the same as the number of input and output parameters of the network, but the neurons' number in the hidden layers is chosen according to the type of problem. During the ANN model training process, each input is multiplied by the value of the weight and then added together; next, a bias, that is connected only to the hidden layer and output layer (usually considered a non-zero constant), is added to the neuron. The activity of the neuron as the output is determined as follows:

$$net_j = \sum_{i=1}^{n} w_{ij} x_i + b_j \tag{1}$$

where net_j indicates the collection of data about neurons; x_i is the value of the input, and b_j and w_{ij} are the bias and the corresponding weight values, respectively.

In the end, the final outputs are determined using transfer or activation functions, which apply nonlinearity to the ANN model and make it very strong. The transfer functions

typically used in the ANN models, consist of Sigmoid, Gaussian, and Hyperbolic tangent as the nonlinear functions or Step and Rampage as the linear functions. The outputs can be obtained using the following equation:

$$out_j = f\left(net_j\right) \tag{2}$$

where out_j represents the output of jth node and f represents the transfer function.

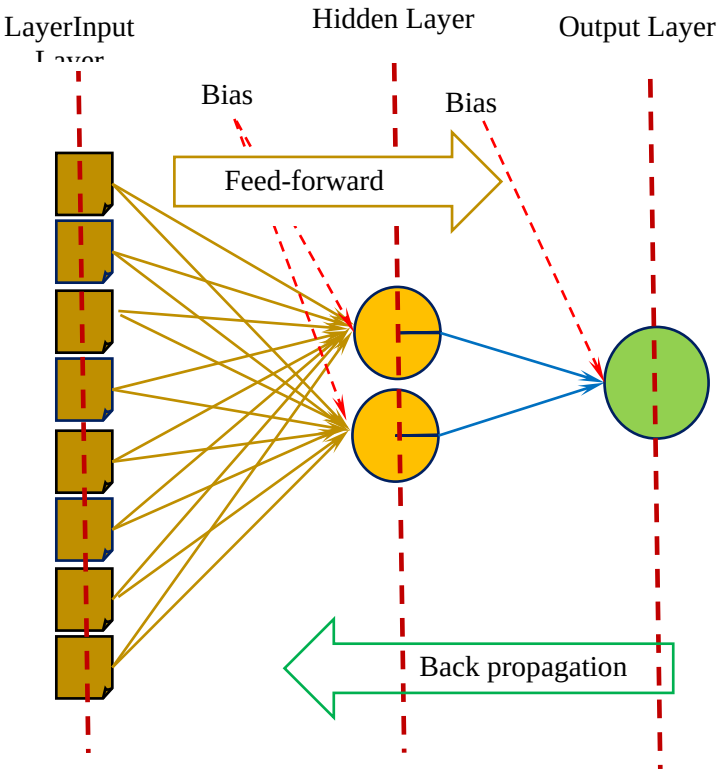

Figure 7. Structure of a shallow neural network

Since ANN is a nonlinear method, optimization algorithms are needed to minimize the cost function. Various algorithms can be used for this purpose, such as scaled conjugate gradient, one-step secant, variable learning rate, Fletcher-Reeves conjugate gradient, Levenberg-Marquardt, and so on. In the current study, the Levenberg-Marquardt (LM) algorithm was employed to train ANN models. This algorithm is based on the Newton method and is very suitable for training the models up to several hundredweights [43, 44]. In previous studies [26-28], its effectiveness in solving various problems has been proven. The LM algorithm is very efficient compared to other methods and in many cases when other back-propagation algorithms diverge, this algorithm converges.

4.2 Developed ANN model for predicting LDB capacity of cellular beams

A two-layer ANN model with one hidden layer was considered for the prediction of the LDB capacity of cellular beams. Based on the studies that have been done so far, this type of network has a good predictive ability to solve common engineering problems [31-34]. Since it is difficult to identify all the variables affecting the ultimate resistance of cellular beams and also some of the effective parameters are strongly related to each other, in this study, eight effective parameters were considered as the model inputs based on the performed parametric study. The initial output and input vectors of the model include one and eight dimensionless variables, respectively:

$$Input = \left\{ \frac{h_w}{b_f}, \frac{t_f}{t_w}, \frac{h_w}{t_w}, \frac{b_f}{2t_f}, \frac{L_b}{r_y}, \frac{h_w}{D}, \frac{S}{D}, \frac{E}{F_y} \right\}$$

$$Output = \left\{ \frac{M_{DB}}{M_p} \right\}$$

where M_{DB} represents the ultimate LDB capacity of cellular steel beams and M_p represents the major axis full plastic moment:

$$M_P = F_y.Z_x \tag{3}$$

where Z_x and F_y represent the plastic section modulus and the yield strength, respectively.

According to these vectors, the input and output layers have eight and one nodes, respectively. Moreover, the neurons' number in the hidden layer has a great effect on the behavior of back-propagation networks. As mentioned before, estimation of the appropriate number of neurons in the hidden layer is usually performed by trial and error technique. Fig. 8 shows the accuracy of the models with 1-10 neurons in their hidden layer. In the figure, *R* is the correlation coefficient and *MSE* is the mean squared error, which is expressed based on the Eqs. (4) and (5):

$$R = \frac{\sum_{i=1}^{N}(y_i - \bar{y})(t_i - \bar{t})}{\sqrt{\sum_{i=1}^{N}(y_i - \bar{y})^2 \sum_{i=1}^{N}(t_i - \bar{t})^2}} \tag{4}$$

$$MSE = \frac{1}{N}\sum_{i=1}^{N}(t_i - y_i)^2 \tag{5}$$

where t_i and $\bar{t}_i$ indicate the target output and the average of target outputs, respectively; and y_i and $\bar{y}_i$ indicate the predicted output and the average of predicted outputs, respectively. Also, *N* indicates the number of samples. It is worth mentioning that although increasing the number of neurons in the hidden layer makes the network more accurate, it also leads to a lengthy and tedious relationship. Therefore, in this study, considering the predictive power and applicability of the ANN-based equation, two neurons in the hidden layer were chosen to estimate the ultimate LDB capacity of cellular I-beams.

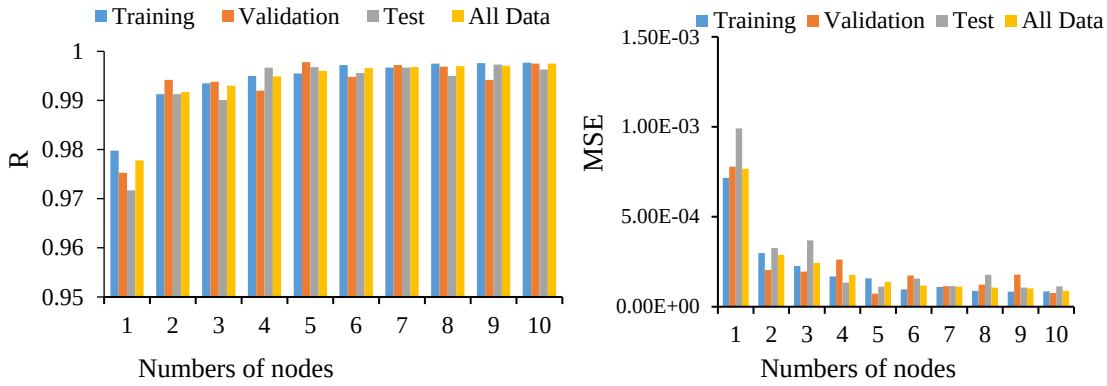

Figure 8. R and MSE values correspond to networks with different numbers of neurons in their hidden layer

Moreover, another problem that can occur during the training process of a neural network is over-fitting. This arises when the network error is small, but as the network is given more information, the error increases. In the current study, to solve the over-fitting problem, the early stop (ES) technique is used. In this technique, a validation dataset is used in such a way that by dividing the database into three datasets of training, after the network starts to over-fit the training data, the validation data error increases for certain steps of iteration, and the network training stops, as well as the biases and weights related to the minimum validation error, are automatically restored. This method increases the predictive power of the network for new samples that have not been used in the training data. Therefore, the database in this paper was divided into three sets: 70% for network training, 15% for validation, and 15% for independent testing. From 660 data vectors, 462 and 99 data vectors were employed for training and validation of the ANN model and the remaining 99 data vectors were employed for model testing. It should be mentioned that the number of data vectors adopted for network training is strongly related to network reliability. Frank and Todeschini [45] proposed that the minimum ratio of the number of all data vectors to the number of input parameters be considered three to make the model acceptable; however, the authors recommended a ratio of five for a more accurate model. In this paper, this ratio, considering 660 data vectors and eight input variables, was equal to 660/8=82.5. Besides, to speed up network learning and to accomplish more accurate results, the input and output variables were standardized according to Eq. (6) and then used in the training process of the ANN model

$$X_{si} = \frac{X_i - Mean}{SD} \tag{6}$$

where X_i indicates the variable value and *Mean* and *SD* indicates the mean and standard deviation of variables, respectively.

Consequently, considering eight input variables and one output variable, a two-layer ANN model, based on the learning algorithm of LM/BP was constructed and trained. The Log-Sigmoid function and the linear transfer function were employed for the hidden and

output layers, respectively. Also, two neurons were used in the hidden layer of the developed model. The toolbox provided in the MATLAB program was used to develop ANNs. The distribution patterns of database variables using frequency histograms are tabulated in Fig. 9.

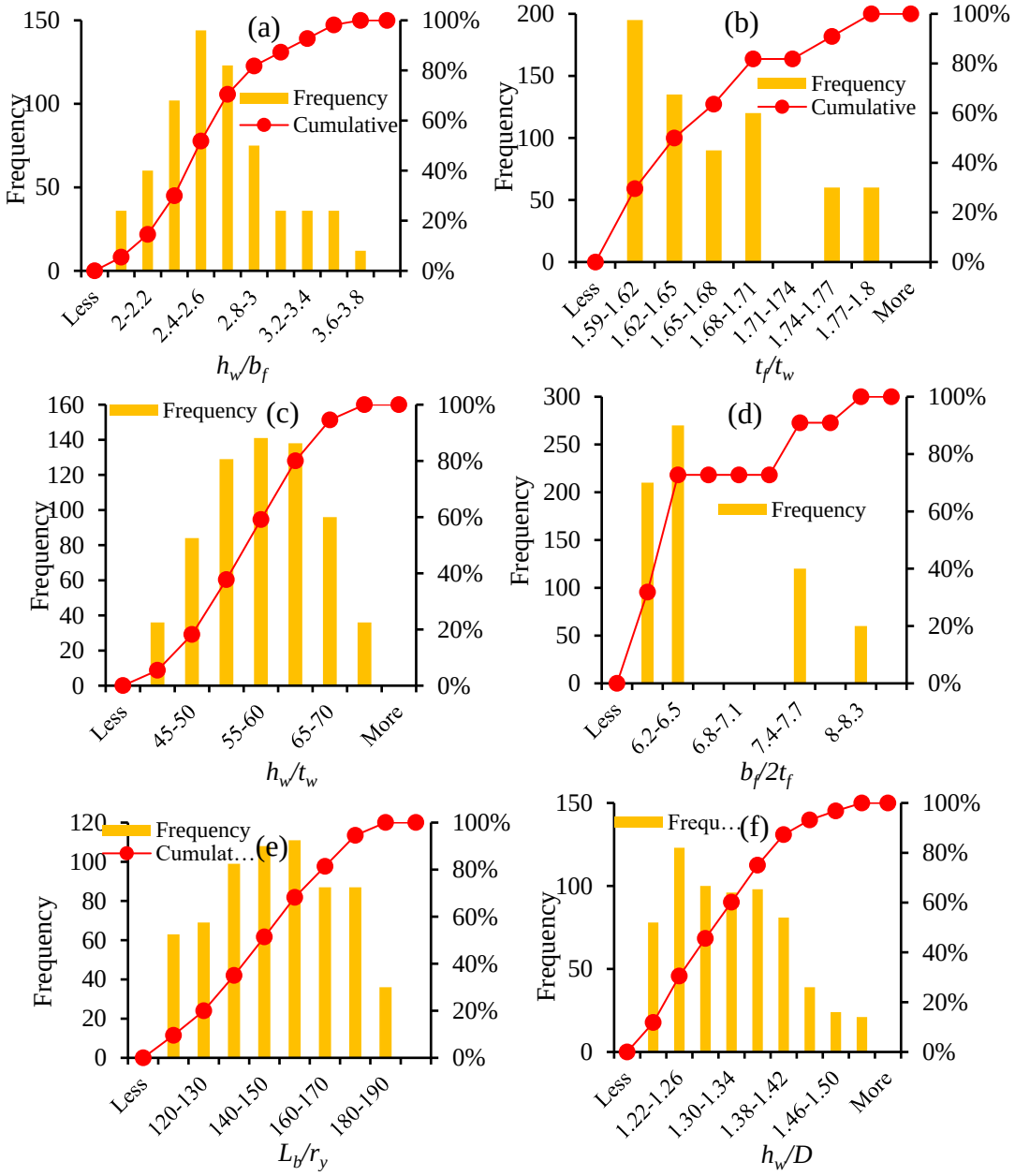

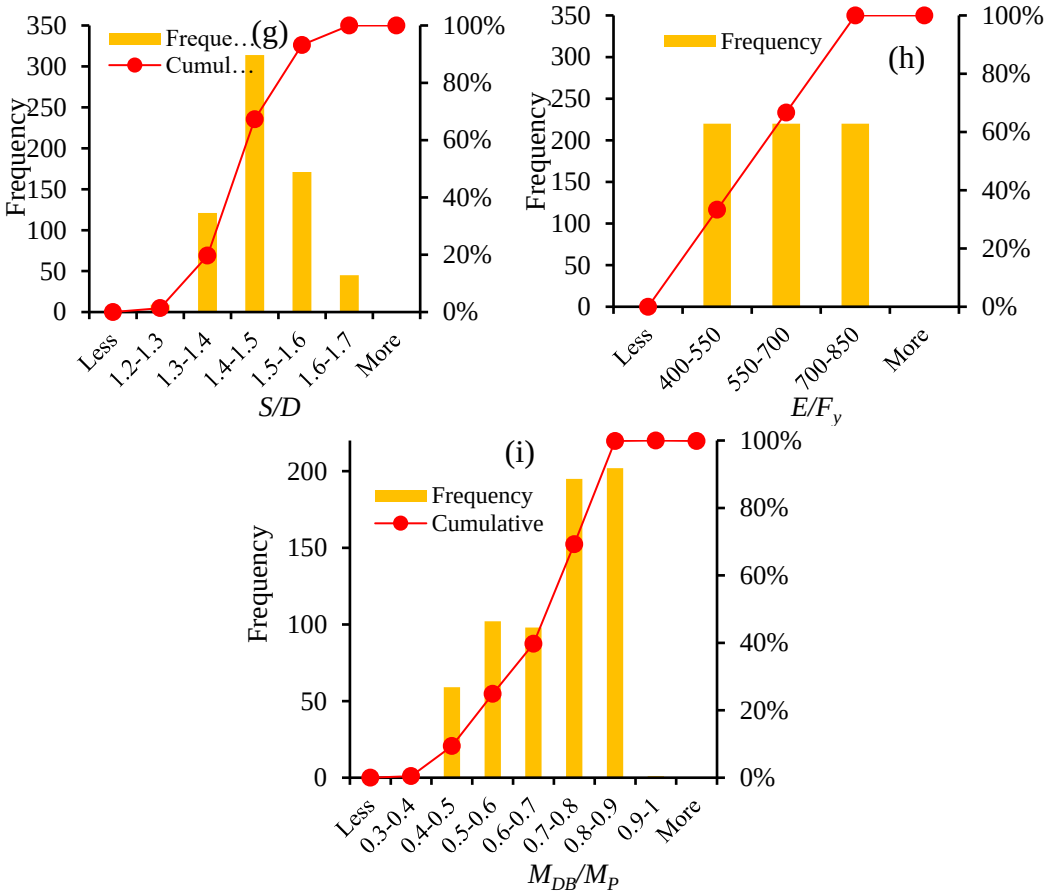

Figure 9. Histograms of the input parameters

4.3 ANN-based formulation

The output of each three-layer network can be stated as follow:

$$output = f_2\left(W_2 \times \left(f_1\left(W_1 \times X + b_1\right)\right) + b_2\right) \tag{7}$$

where W_1 and W_2 represent the weight matrixes of the second and third layers, respectively. As well as b_1 and b_2 represent the bias vectors of the second and third layers, respectively. Also, f_i represents the transfer functions used in these layers. Finally, according to the above relation, the following formula is offered to predict the LDB capacity of cellular beams:

$$M_{DB} = \left(0.4697 - \frac{0.673}{1+e^{-\beta_1}} + \frac{0.5636}{1+e^{-\beta_2}}\right) M_p \tag{8}$$

$$\beta_1 = -0.1282\times\left(\frac{h_w}{b_f}\right)-1.5164\times\left(\frac{t_f}{t_w}\right)+0.0225\times\left(\frac{h_w}{t_w}\right)-0.2015\times\left(\frac{b_f}{2t_f}\right)-0.008\times\left(\frac{L_b}{r_y}\right)-2.5427\times\left(\frac{h_w}{D}\right)-0.3273\times\left(\frac{S}{D}\right)$$
$$+0.0018\times\left(\frac{E}{F_y}\right)+5.5322$$

$$\beta_2 = -0.3147\times\left(\frac{h_w}{b_f}\right)-1.6039\times\left(\frac{t_f}{t_w}\right)+0.0002\times\left(\frac{h_w}{t_w}\right)-0.2491\times\left(\frac{b_f}{2t_f}\right)-0.0545\times\left(\frac{L_b}{r_y}\right)-1.4926\times\left(\frac{h_w}{D}\right)-0.1312\times\left(\frac{S}{D}\right)$$
$$+0.0096\times\left(\frac{E}{F_y}\right)+10.7905$$

This should be noted that the scope of application of the formula is determined based on the boundary conditions considered in this study and also according to the range of input variables, which is reported in Table 2. In order to expand the application of Eq. (8), more research should be accomplished with different support and load conditions, moreover, more numerical or experimental studies are required for generalizing the approach.

5. PERFORMANCE ANALYSIS AND COMPARATIVE STUDY

In order to estimate the efficiency and accuracy of the proposed formula, four parameters comprising correlation coefficient (*R*), mean squared error (*MSE*), mean absolute error (*MAE*), and absolute percentage error (*Err*) was adopted. The equations for *R* and *MSE* were previously stated in Eqs. 4 and 5, *MAE* and *Err* are also calculated according to the following equations:

$$MAE = \frac{1}{N}\sum_{i=1}^{N}\left|y_i - t_i\right| \tag{9}$$

$$Err_i = \frac{\left|y_i - t_i\right|}{t_i}\times 100 \tag{10}$$

where t_i , y_i , $\overline{t_i}$, $\overline{y_i}$ and N are the same parameters used in Eqs. 4 and 5.

Table 3 presents the performance ability of the obtained equation-based ANN, and those proposed by AISC, AS4100, and EC3. Here, the *R*, *MSE*, and *MAE* were introduced as the target-measured parameters to illustrate the capability of the presented equation. Based on them, the ANN formula involves a proper precision for assessing the LDB strength of cellular steel beams in comparison with the AISC, AS4100, and EC3 code provisions. In the testing data set that did not participate in the model development, the *R*-based-ANN was justified as 0.9912, compared to 0.9012, 0.9445, and 0.8915 for the AISC, AS4100, and EC3 codes, respectively.

Table 3: The introduced statistics parameters for M_{DB}/M_P calculation

Method	Training			Validation			Testing		
	R	MSE	MAE	R	MSE	MAE	R	MSE	MAE
Proposed equation	0.9913	0.0003	0.0120	0.9943	0.0002	0.0104	0.9912	0.0003	0.0143
AS4100	0.8887	0.0134	0.1073	0.8879	0.0136	0.1068	0.9012	0.0128	0.1045
AISC	0.9298	0.0081	0.0683	0.9221	0.0092	0.0745	0.9445	0.0083	0.0725
EC3	0.8765	0.0174	0.1197	0.8742	0.0185	0.1241	0.8915	0.0169	0.1187

Furthermore, the errors arising from AISC, AS4100, EC3 codes, and by the developed formula are tabulated in Figs. 10, 11, and 12. It is clear that the new formula-based-ANN approach provides more precise predictions for the LDB moment of cellular steel beams among others. Besides, another comparison between the predictions of the new formula-based-ANN approach and the existing code provisions was established in Fig. 13. Based on Fig. 13 presentation, a model containing suitable accuracy includes the actual to predicted values ratio close to one. This figure shows that the distribution of the predicted values for the ANN-based formula gives more accuracy than others.

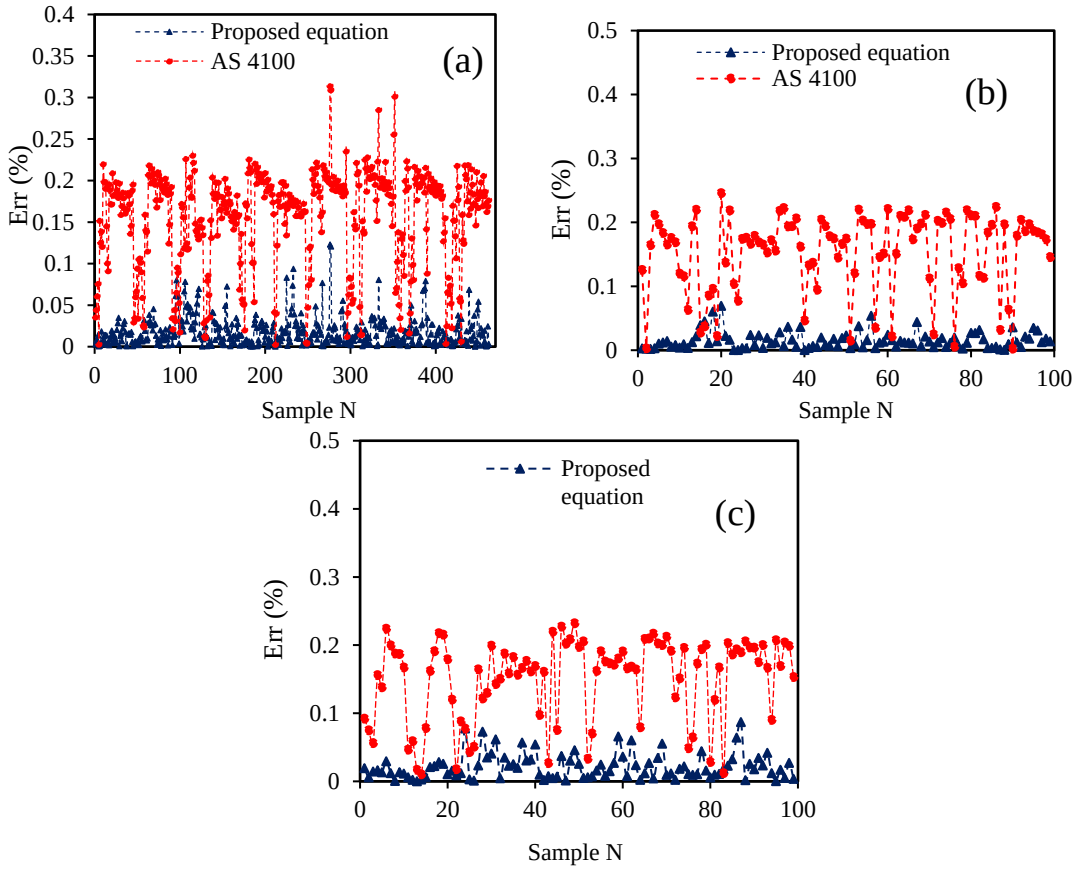

Figure 10. Predictions based on the AS4100 code vs proposed formula: (a) training data, (b) validation data, (c) testing data

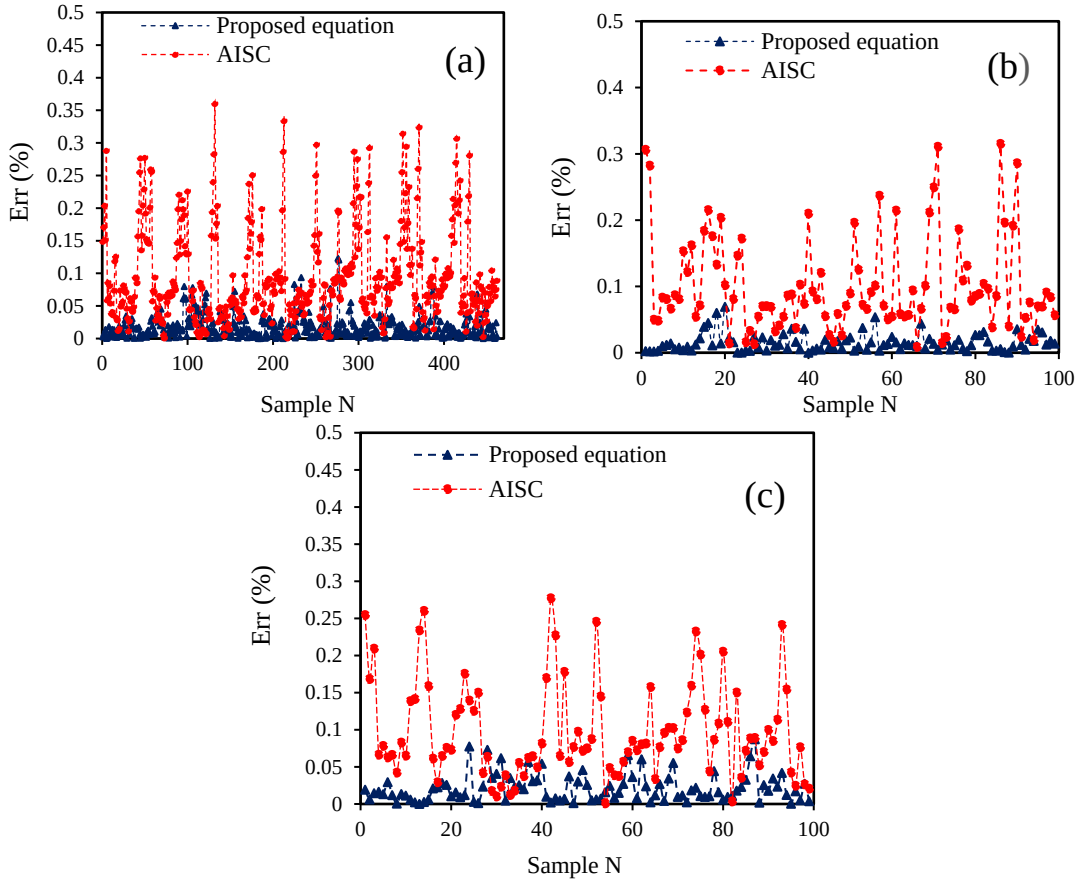

Figure 11. Predictions based on the AISC code vs proposed equation: (a) training data, (b) validation data, (c) testing data

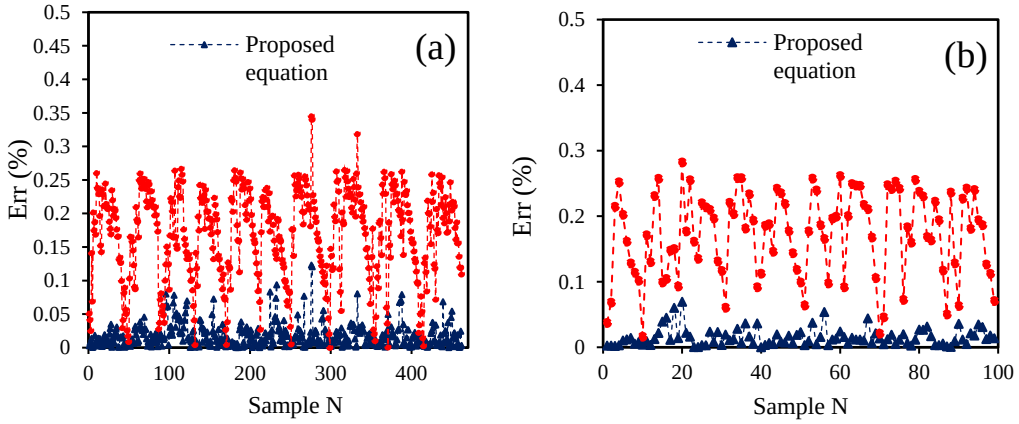

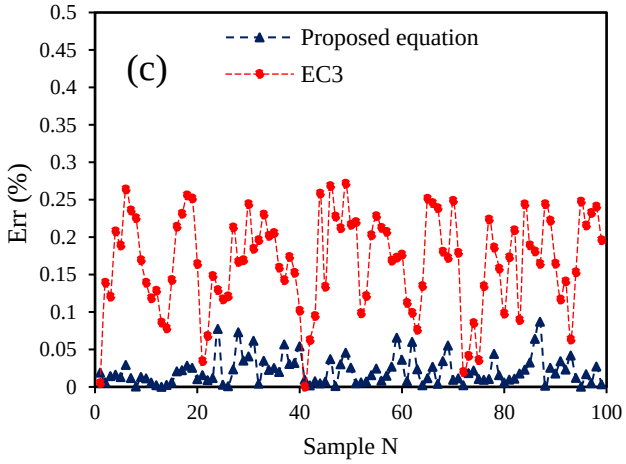

Figure 12. Predictions based on the EC3 code vs proposed equation: (a) training data, (b) validation data, (c) testing data

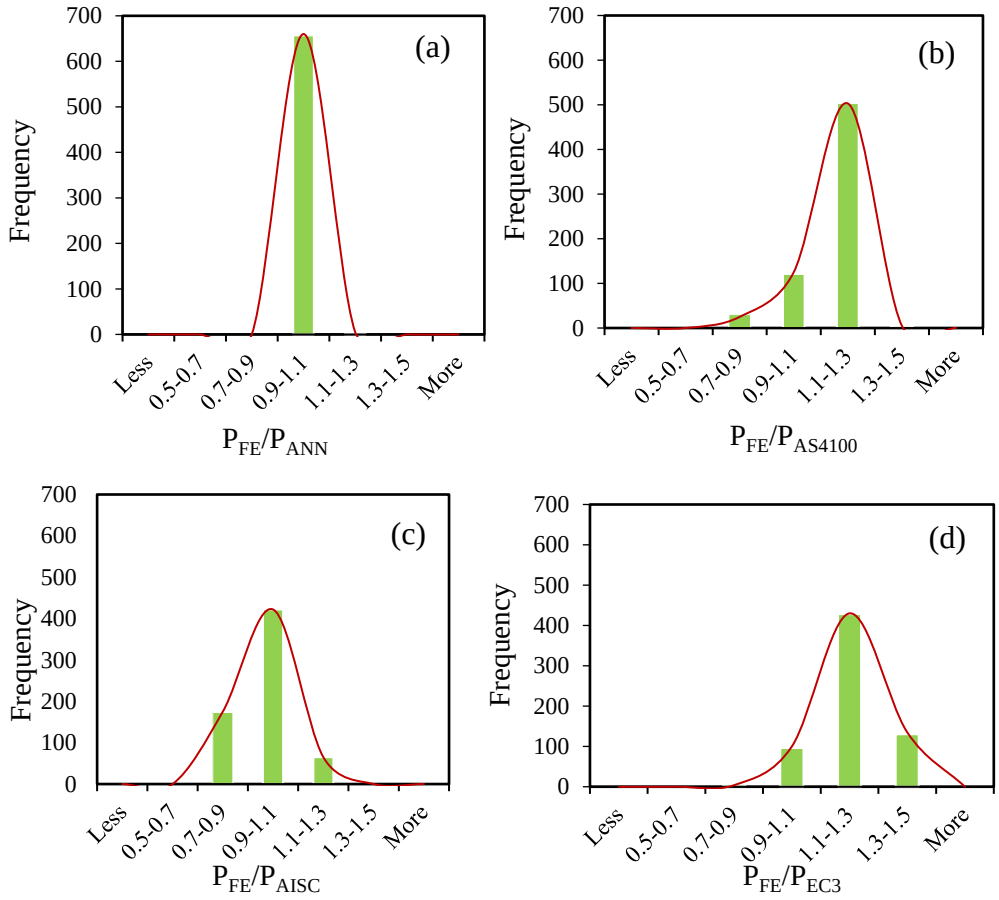

Figure 13. A comparison between the ANN-based formula and design codes: (a) Proposed formula (b) AS4100 (c) AISC (d) EC3

6. SENSITIVITY ANALYSIS

In this section, sensitivity analysis is developed to determine the importance of each of the input parameters in the ANN model. To do this, Garson's algorithm was used for determining the significance of the input parameters according to Ref. [46]. As clarified in Fig. 14, For a model comprising eight nodes in the input layer (1-8), two nodes in the hidden layer (A and B), and one node in the output layer (O), the steps of the algorithm, can be expressed as follows:

- Calculate the contribution of inputs through input-hidden-output connections (e.g. $C_{A1}=W_{A1}\times W_{oA}$).
- Calculate the relative contributions of inputs (e.g. $r_{A1}=|C_{A1}|/|C_{A1}+C_{A2}+\ldots+C_{A8}|$).
- Calculate the sum of relative contributions (e.g. $S_1=r_{A1}+r_{B1}$).
- Calculate the relative importance of inputs (e.g. $I_1=S_1/(S_1+S_2+\ldots+S_8)$).

Fig. 15 presents the used input variable's significance ~~of~~ in the ANN model. From Fig. 15, the E/F_y and L_b/r_y parameters show the most effective variables for the assessment of the LDB strength t of cellular steel beams, respectively.

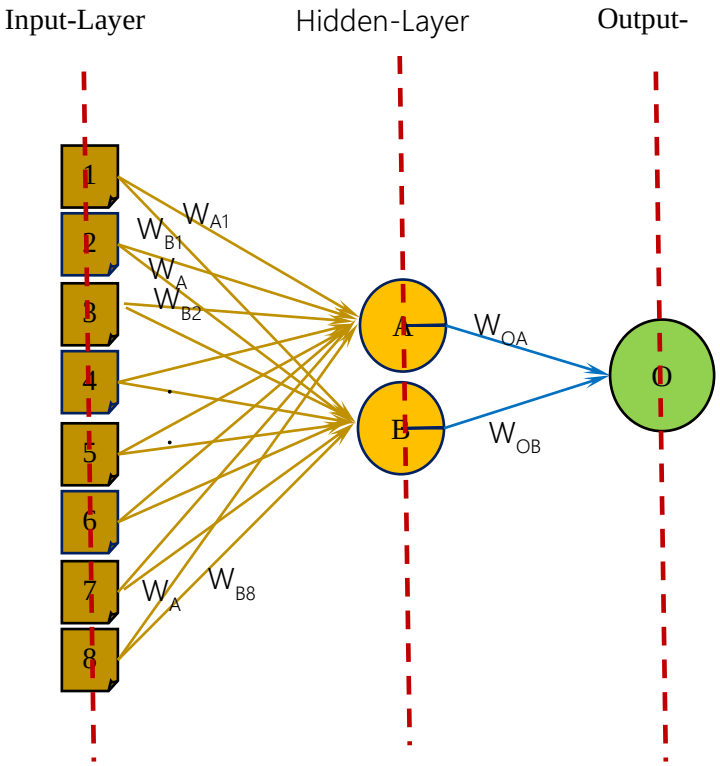

Figure 14. Garson's algorithm procedure using ANN

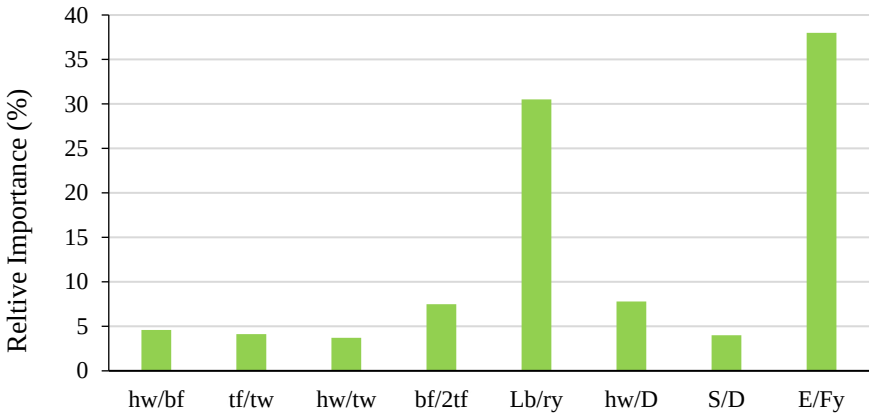

Figure 15. Independent variable importance in the ANN model

7. CONCLUSIONS

A series of FEA models were performed to evaluate the ultimate LDB resistance of the cellular steel I-shaped beams. The numerical study included 660 samples of cellular steel beams that were different in parameters such as cross-sectional dimensions, opening dimensions, yield strength of steel, and beam length. At the first, for each sample, the ultimate capacity and the failure mode were calculated utilizing the reliable and verified FEA model generation. Then, the ultimate capacity values predicted by AISC, AS4100, and EC3 code provisions were compared with the FEA results. Based on the outcomes, the mentioned codes offered unsafe and un-conservative estimations for the majority of specimens. Consequently, in the next step, it was tried to develop an accurate ANN model to provide a new precise equation to assess the maximum moment capacity of cellular steel beams subjected to LDB mode failure. The ANN-based empirical formula shows excellent accuracy, and practical engineers can use this formulation for calculating the LDB moment capacity of cellular steel beams. In the end, a sensitivity analysis was also performed to introduce the more effective variables on the LDB capacity of cellular beams.

On behalf of all authors, the corresponding author states that there is no conflict of interest.

REFERENCES

1. Sharifi Y, Moghbeli A, Hosseinpour M, Sharifi H. Neural networks for lateral torsional buckling strength assessment of cellular steel I-beams, *Adv Struct Eng* 2019; **22**(9): 2192-2202.
2. Sharifi Y, Moghbeli A, Hosseinpour M, Sharifi H. Study of neural network models for the ultimate capacities of cellular steel beams, *Iran J Sci Technol Trans Civil Eng* 2019. https://doi.org/10.1007/s40996-019-00281-z.

3. Sharifi Y, Hosseinpour M, Moghbeli A, Sharifi H. Lateral torsional buckling capacity assessment of castellated steel beams using artificial neural networks, *Int J Steel Struct* 2019, **19**: 1408-20.
4. Erdal F, Saka MP. Ultimate load carrying capacity of optimally designed steel cellular beams, *J Constr Steel Res* 2013; 80: 355-68.
5. Nseir J, Lo M, Sonck D, Somja H, Vassart O, Boissonnade N. Lateral torsional buckling of cellular beams, in: *Proceedings of the Structural Stability Research Council Annual Stability Conference (SSRC2012)*, Grapevine, Texas, 2012.
6. Sonck D. *Global Buckling of Castellated and Cellular Beams and Columns* (Ph. d. dissertation), Ghent University, Belgium, 2014.
7. Ellobody E. Nonlinear analysis of cellular beams under combined buckling modes, *Thin-Walled Struct* 2012; 52: 66-79.
8. Tsavdaridis KD, D'Mello C. Web buckling study of the behaviour and strength of perforated steel beams with different novel web opening shapes, *J Constr Steel Res* 2011; **67**: 1605-20.
9. Chung KF, Lawson RM. Simplified design of composite beams with large web openings to Eurocode 4, *J Constr Steel Res* 2001; 57: 135-63.
10. Lawson RM, Oshatogbe D, Newman GM. Design of FABSEC Cellular Beams in Non-Composite and Composite Applications for Both Normal Temperature and Fire Engineering Conditions, Fabsec Limited Publication, 2006 (Cellular Beam Software: FBeam 2006 design guide), UK.
11. Panedpojaman P, Thepchatri T, Limkatanyu S. Novel design equations for shear strength of local web-post buckling in cellular beams, *Thin-Walled Struct* 2014; **76**: 92-104.
12. Panedpojaman P, Thepchatri T, Limkatanyu S. Novel simplified equations for Vierendeel design of beams with (elongated) circular openings, *Constr Steel Res* 2015; **112**: 10–21.
13. Sweedan AMI. Elastic lateral stability of I-shaped cellular beams, *J Constr Steel Res* 2011; **67**: 151–163.
14. El-Sawy KM, Sweedan AMI, Martini MI. Moment gradient factor of cellular beams under inelastic flexure, *J Constr Steel Res* 2014; **98**: 20–34.
15. Sonck D, Belis J. Lateral–torsional buckling resistance of cellular beams, *J Constr Steel Res* 2015; **105**: 119-28.
16. Tohidi S, Sharifi Y. Empirical modeling of distortional buckling strength of half-through bridge girders via stepwise regression method, *Adv Struct Eng* 2015, **18**(9): 1383-97.
17. Tohidi S, Sharifi Y. Neural networks for inelastic distortional buckling capacity assessment of steel I-beams, *Thin-Wall Struct* 2015; **94**(9): 359-71.
18. Tohidi S, Sharifi Y. Restrained distortional buckling capacity of half through bridge girders, *IES J Part A: Civil Struct Eng* 2014, 7(3): 163-73. DOI:10.1080/19373260.2014.921400.
19. Tohidi S, Sharifi Y. A new predictive model for restrained distortional buckling strength of half-through bridge girders using artificial neural network, *KSCE J Civil Eng* 2014; **10**(3): 325–50. DOI:10.18057/IJASC.2014.10.3.5.

20. Sharifi Y, Tohidi S. Lateral-torsional buckling capacity assessment of web opening steel girders by artificial neural networks–elastic investigation, *Front Struct Civil Eng* 2014, **8**(2): 167–177. DOI: 10.1007/s11709-014-0236-z
21. Bradford MA. Distortional buckling of elastically restrained cantilevers, *J Construct Steel Res* 1998; **47**: 3–18.
22. Zirakian T. Elastic distortional buckling of doubly symmetric I-shaped flexural members with slender webs, *J Construct Steel Res* 2008; **46**: 466-75.
23. Zirakian T, Showkati H. Distortional buckling of cellular beams, *J Construct Steel Res* 2006; **62**: 863–71.
24. Kaveh A, Shokohi F. Cost optimization of end-filled castellated beams using meta-heuristic algorithms, *Int J Optim Civil Eng* 2015; **5**(3) 329-51.
25. Sharifi Y. Hosseinpour M. Adaptive neuro-fuzzy inference system and stepwise regression for compressive strength assessment of concrete containing metakaolin, *Int J Optim Civil Eng* 2019; **9**(2): 251-72.
26. Kaveh A, Khalegi HA. Prediction of strength for concrete specimens using artificial neural network, *Asian J Civil Eng* 2000; **2**(2): 1-13.
27. Kaveh A, Rahimi HA. Bondarabady, Wavefront reduction using graphs, neural networks and genetic algorithm, *Int J Numer Meth Eng* 2004; **60**: 1803-15.
28. Rofooei FR, Kaveh A, Masteri Farahani F. Estimating the vulnerability of concrete moment resisting frame structures using artificial neural networks, *Int J Operat Res* 2011; 3(1): 433-48.
29. Hosseinpour M, Sharifi H, Sharifi Y. Stepwise regression modeling for compressive strength assessment of mortar containing metakaolin, *Int J Modell Simulat* 2018; **38**(4): pp. 207-15.
30. Kaveh A, Raiessi Dehkordi M. RBF and BP neural networks for the analysis and design of domes, *Int J Space Struct* 2003; **18**(3): 181-94.
31. Kaveh A, Fazel-Dehkordi D, Servati H. Prediction of moment-rotation characteristic for saddle-like connections using BP neural networks, *Asian J Civil Eng* 2001; 2(1): 11-30.
32. Kaveh A, Gholipour Y, Rahami H. Optimal design of transmission towers using genetic algorithm and neural networks, *Int J Space Struct* 2008; **23**(1): 1-19.
33. Kaveh A, Elmieh R, Servati H. Prediction of moment-rotation characteristic for semi-rigid connections using BP neural networks, *Asian J Civil Eng* 2001; **2**(2): 131-42.
34. Hosseinpour M, Sharifi Y, Sharifi H, Neural network application for distortional buckling capacity assessment of castellated steel beams, *Struct* 2020; **27**: 1174-83. https://doi.org/10.1016/j.istruc.2020.07.027.
35. ABAQUS standard user's manual. Hibbitt, Karlsson and Sorensen, Inc. Version 6.8-1. USA 2008; **1-3**.
36. AISC. Specification for structural steel buildings. American institute for steel construction. Reston (Chicago, Illinois, USA): ANSI/AISC 360-05; 2005.
37. Australian Standards AS4100. Steel structures. Sydney (Australia): Standards Australia, AS4100-1998; 1998.
38. Eurocode 3. Design of Steel Structures Part 1–1: General Rules and Rules for Buildings, European Committee for Standardization (ECS), Brussels, Belgium, 2005.

39. Zirakian T, Showkati H. Experiments on distortional buckling of I-beams, *J Struct Eng ASCE* 2007; **133**(7): 1009–17.
40. Bradford MA, Wee A. Analysis of buckling tests on beams on seat supports, *J Constr Steel Res* 1994; **28**: 227–42.
41. Cybenko J. Approximations by super positions of a sigmoidal function, *Math Control Signal Syst* 1989, **2**: 303–14.
42. Hristev RM. The ANN book. GNU public license, 1998.
43. Marquardt D. An algorithm for least squares estimation of non-linear parameters, *J Soc Ind Appl Math* 1963; **11**: 431–41.
44. Hagan MT, Menhaj MB. Training feed forward networks with the Marquardt algorithm, *IEEE Transact Neural Net* 1994; **5**(6): 861-7.
45. Frank IE, Todeschini R. The data analysis handbook, Amsterdam, Elsevier, 1994.
46. Garson GD. Interpreting neural-network connection weights, *AI Expert* 1991, 6: 47–51.